Frequency Domain Analysis of Jitter Amplification in Clock Channels

Fangyi Rao
Agilent Technologies, Inc.
Santa Clara, CA
fangyi_rao@agilent.com

Sammy Hindi
Juniper Networks
Sunnyvale, CA
shindi@juniper.net

***Abstract*—Clock channel jitter amplification factor in terms of transfer function or S-parameters is derived. Amplification is shown to arise from smaller attenuation in jitter lower sideband than in the fundamental. Amplification scaling with loss is obtained analytically.**

***Index Terms*—jitter, amplification, loss.**

I. Introduction

High speed interconnect performance is increasingly influenced by jitter as data rate advances. The amount of jitter is modulated by channel dispersion as signals propagate in the system. It is observed in both measurements and simulations that jitter can be amplified by a lossy channel even when the channel is linear, passive and noiseless [1]-[4]. The mechanism of jitter amplification is discussed in terms of channel impulse/step response in [2]-[4]. In particular, duty-cycle-distortion (DCD) and random jitter (RJ) amplifications in clock signals are shown to scale uniquely with channel loss [2], indicating that loss is responsible for the effect.

In this paper jitter amplification in clock channels is analyzed analytically in frequency domain. The advantage of using clock signals is that the periodicity of the 1010 clock pattern eliminates the inter-symbol-interference (ISI) jitter so jitter at the channel output is entirely induced by input jitter. A phase modulation (PM) approach is employed to derive the jitter transfer function and amplification factors in terms of signal transfer function or channel S-parameters for sinusoidal jitter (SJ), DCD and RJ. Results show that jitter amplification is the consequence of smaller attenuation in the jitter lower sideband (LSB) than in the fundamental. The scaling of DCD and RJ amplifications with channel loss is explained by using an approximate loss model. It is shown that jitter is amplified by lossy channels at any frequency below Nyquist and the effect grows exponentially with jitter frequency and data rate. The theory is verified by simulation results.

II. Jitter Transfer function and amplification

In lossy channels high order harmonics are heavily attenuated and the 1010 clock pattern can be approximated by a sinusoidal wave with frequency at one half of the data rate. Jitter in the input clock signal, v_{in}, can be represented by phase modulation as

$$v_{in}(t) = A\cos[\omega_0 t + \theta_0 + \phi(t)] \tag{1}$$

where ω_0 is the fundamental frequency of the clock signal, θ_0 a constant phase offset, and ϕ the phase modulation that represents jitter. When ϕ is small Eq. 1 can be linearized.

$$\begin{aligned} v_{in}(t) \approx \frac{A}{2}[&\exp(j\omega_0 t + j\theta_0) + j\phi(t)\exp(j\omega_0 t + j\theta_0) \\ &+ \exp(-j\omega_0 t - j\theta_0) - j\phi(t)\exp(-j\omega_0 t - j\theta_0)] \end{aligned} \tag{2}$$

Consider a sinusoidal jitter at frequency ω.

$$\phi(t) = \phi(\omega)\exp(j\omega t) + \phi(\omega)^* \exp(-j\omega t) \tag{3}$$

Substitution of Eq. 3 into Eq. 2 yields

$$\begin{aligned} v_{in} = \frac{A}{2}\{&\exp(j\omega_0 t + j\theta_0) \\ &+ j\phi(\omega)\exp[j(\omega+\omega_0)t + j\theta_0] \\ &+ j\phi(\omega)^* \exp[j(-\omega+\omega_0)t + j\theta_0] \\ &+ \exp(-j\omega_0 t - j\theta_0) \\ &- j\phi(\omega)\exp[j(\omega-\omega_0)t - j\theta_0] \\ &- j\phi(\omega)^* \exp[j(-\omega-\omega_0)t - j\theta_0]\} \end{aligned} \tag{4}$$

Assume the signal transfer function of the channel is $H(\omega)$. The output signal, v_{out}, is given by

$$\begin{aligned} v_{out}(t) = \frac{A}{2}\{&H(\omega_0)\exp(j\omega_0 t + j\theta_0) \\ &+ jH(\omega+\omega_0)\phi(\omega)\exp[j(\omega+\omega_0)t + j\theta_0] \\ &+ jH(-\omega+\omega_0)\phi(\omega)^* \exp[j(-\omega+\omega_0)t + j\theta_0] \\ &+ H(-\omega_0)\exp(-j\omega_0 t - j\theta_0) \\ &- jH(\omega-\omega_0)\phi(\omega)\exp[j(\omega-\omega_0)t - j\theta_0] \\ &- jH(-\omega-\omega_0)\phi(\omega)^* \exp[j(-\omega-\omega_0)t - j\theta_0]\} \\ = \frac{A}{2}&H(\omega_0)\exp(j\omega_0 t + j\theta_0)[1 + j\psi_+(t)] \\ &+ \frac{A}{2}H(-\omega_0)\exp(-j\omega_0 t - j\theta_0)[1 - j\psi_-(t)] \end{aligned} \tag{5}$$

where ψ_+ and ψ_- are defined as

$$\psi_+(t)=\frac{H(\omega+\omega_0)}{H(\omega_0)}\phi(\omega)e^{j\omega t}+\frac{H(-\omega+\omega_0)}{H(\omega_0)}\phi(\omega)^* e^{-j\omega t}$$
$$\psi_-(t)=\frac{H(\omega-\omega_0)}{H(-\omega_0)}\phi(\omega)e^{j\omega t}+\frac{H(-\omega-\omega_0)}{H(-\omega_0)}\phi(\omega)^* e^{-j\omega t} \quad (6)$$

Notice that $\psi_+=\psi_-^*$. For small ϕ Eq. 5 can be rewritten as

$$v_{out}(t)\approx A\,|H(\omega_0)|\exp[-\mathrm{Im}\psi_+(t)]\cos\left[\omega_0 t+j\theta_0+j\angle H(\omega_0)+j\,\mathrm{Re}\psi_+(t)\right] \quad (7)$$

where $\mathrm{Re}\psi_+$ and $\mathrm{Im}\psi_+$ denote real and imaginary parts of ψ_+, respectively. Phase modulation in the output signal is given by the $\mathrm{Re}\psi_+$ term in Eq. 7 as

$$\phi_{out}(t)=\mathrm{Re}\,\psi_+(t)=\left|\frac{H(\omega+\omega_0)}{H(\omega_0)}+\frac{H(\omega-\omega_0)}{H(-\omega_0)}\right||\phi(\omega)|\cos[\omega t+\angle\phi(\omega)+\gamma] \quad (8)$$

where γ is the phase of $[H(\omega+\omega_0)/H(\omega_0)+H(\omega-\omega_0)/H(-\omega_0)]$. Equation 8 shows that a SJ is induced in the output by the input SJ. The jitter transfer function, defined as the ratio of amplitude between output and input SJ, is obtained as

$$F_{SJ}(\omega)=\frac{1}{2}\left|\frac{H(\omega+\omega_0)}{H(\omega_0)}+\frac{H(\omega-\omega_0)}{H(-\omega_0)}\right| \quad (9)$$

Equation 9 describes the relation between jitter amplification and channel dispersion. In a lossy channel, $H(\omega)$ decays with frequency exponentially. The lower sideband of PM at $\omega-\omega_0$ is attenuated less than the carrier is, producing a gain in the output PM that leads to jitter amplification. Equation 9 demonstrates that the amplification, dominated by the $\omega-\omega_0$ term, arises primarily from the attenuation difference between the LSB and the fundamental. Equalizations that compensate high frequency loss reduce the amplification effect.

It is worth pointing out that input jitter also causes amplitude modulation in the output signal, as shown by the $\mathrm{Im}\psi_+$ term in Eq. 7, resulting in eye height impairment.

Amplification factors of DCD and RJ can be derived from Eq. 9. DCD is equivalent to SJ at frequency ω_0 and the amplification factor is given by Eq. 9 as

$$F_{DCD}=\frac{1}{2}\left|\frac{H(2\omega_0)}{H(\omega_0)}+\frac{H(0)}{H(-\omega_0)}\right| \quad (10)$$

Note that the LSB of PM becomes a DC offset when the modulation frequency equals ω_0. Equation 10 shows that DCD amplification is caused by the attenuation difference between the DC component introduced by DCD and the fundamental in lossy channels, as pointed out in [1].

RJ in the input signal is assumed to be white noise and its averaged power is provided by the integration of the power spectral density (PSD) within the jitter Nyquist frequency, which equals ω_0.

$$<\phi(t)^2>=\int_{-\omega_0}^{\omega_0}d\omega C=2C\omega_0 \quad (11)$$

where C is the constant input RJ PSD. The output RJ power is given by the jitter transfer function and C as

$$<\phi_{out}(t)^2>=2C\int_0^{\omega_0}d\omega F_{SJ}(\omega)^2 \quad (12)$$

The RJ amplification factor, defined as the RMS ratio between output and input RJ, is

$$F_{RJ}=\sqrt{\frac{<\phi_{out}(t)^2>}{<\phi(t)^2>}}=\sqrt{\frac{1}{4\omega_0}\int_0^{\omega_0}d\omega\left|\frac{H(\omega+\omega_0)}{H(\omega_0)}+\frac{H(\omega-\omega_0)}{H(-\omega_0)}\right|^2} \quad (13)$$

When impedance mismatch in the channel is negligible, $H(\omega)$ in Eqs. 9, 10 and 13 can be replaced by the channel forward S-parameter.

It can be shown that Eq. 9 is equivalent to the jitter transfer function expressed in terms of impulse response presented in [3] and [4]. As discussed in [3] and [4], the input clock signal can be represented by a 1010 square wave. The output signal is calculated by linear superposition as

$$v_{out}(t)=\sum_{l=even}R(t-lT-\tau_l^{in})-\sum_{m=odd}R(t-mT-\tau_m^{in}) \quad (14)$$

where R(t) is the channel step response, T the unit interval of the clock signal, and τ^{in}_n the input jitter at the n-th bit. When the input jitter is zero, there is no jitter in the output due to the periodicity of the clock pattern. For a given delay t_d, v_{out} crosses the same value at $t = nT+t_d$ for any integer n. With the presence of input jitter, induced jitter in v_{out} can be measured by the crossing time shift. The output jitter at the n-th crossing is obtained by linearizing Eq. 14 at $nT+t_d$ as

$$\tau_n^{out}=\frac{\sum_m(-1)^m h(nT+t_d-mT)\tau_m^{in}}{\sum_m(-1)^m h(nT+t_d-mT)} \quad (15)$$

where h = dR/dt, which is the channel impulse response. For SJ at frequency ω with amplitude Λ, $\tau^{in}_m=\Lambda\cos(\omega mT)$ and Eq. 15 becomes

$$\tau_n^{out}=\frac{\Lambda}{2}\frac{\sum_m h(nT+t_d+mT)[e^{-j(\omega+\omega_0)mT}+e^{j(\omega-\omega_0)mT}]}{\sum_m h(nT+t_d+mT)e^{-j\omega_0 mT}}=\frac{\Lambda}{2}\frac{\tilde{H}_{nT+td}(\omega+\omega_0)+\tilde{H}_{nT+td}(-\omega+\omega_0)}{\tilde{H}_{nT+td}(\omega_0)} \quad (16)$$

in which identity $(-1)^m = \exp(-j\omega_0 mT)$ is applied and $\tilde{H}_v(\omega)$ is the discrete-time-Fourier-transform (DTFT) of h(t+ν). With the use of the relation between DTFT and Fourier transform Eq. 16 is rewritten in terms of H(ω) as

$$\tau_n^{out} = \frac{\Lambda}{2}\frac{\sum_{k=odd} H(\omega + k\omega_0)\exp[\,j(\omega + k\omega_0)t_d\,]}{\sum_{k=odd} H(k\omega_0)\exp(\,jk\omega_0 t_d\,)}\exp(\,j\omega nT) + \frac{\Lambda}{2}\frac{\sum_{k=odd} H(-\omega + k\omega_0)\exp[\,j(-\omega + k\omega_0)t_d\,]}{\sum_{k=odd} H(k\omega_0)\exp(\,jk\omega_0 t_d\,)}\exp(-j\omega nT) \quad (17)$$

where identity $\exp(jk\omega_0 nT) = (-1)^n$ for odd integer k is used. Notice that the first term in Eq. 17 is the complex conjugate of the second term. Thus,

$$\tau_n^{out} = \Lambda\left|\frac{\sum_{k=odd} H(\omega + k\omega_0)\exp[\,j(\omega + k\omega_0)t_d\,]}{\sum_{k=odd} H(k\omega_0)\exp(\,jk\omega_0 t_d\,)}\right|\cos(\omega nT + \alpha) \quad (18)$$

where α is the phase of the coefficient of exp(jωnT) in Eq. 17. The jitter transfer function in the square wave representation is obtained as

$$F_{SJ}(\omega) = \left|\frac{\sum_{k=odd} H(\omega + k\omega_0)\exp[\,j(\omega + k\omega_0)t_d\,]}{\sum_{k=odd} H(k\omega_0)\exp(\,jk\omega_0 t_d\,)}\right| \quad (19)$$

For lossy channels high order harmonics in Eq. 19 can be ignored. Moreover, by choosing t_d to be the phase delay of H at ω_0, $H(\omega_0)\exp(j\omega_0 t_d)$ and $H(-\omega_0)\exp(-j\omega_0 t_d)$ in the denominator are both real and equal to each other. Thus,

$$F_{SJ}(\omega) \approx \frac{1}{2}\left|\frac{H(\omega + \omega_0)\exp[\,j(\omega + \omega_0)t_d\,]}{H(\omega_0)\exp(\,j\omega_0 t_d\,)} + \frac{H(\omega - \omega_0)\exp[\,j(\omega - \omega_0)t_d\,]}{H(-\omega_0)\exp(-j\omega_0 t_d\,)}\right| \quad (20)$$

Equation 20 is identical to Eq. 9. As expected, the square wave formulation converges to the sinusoidal wave formulation when high order harmonics are neglected.

III. SCALING OF DCD AND RJ AMPLIFICATIONS

The scaling of DCD and RJ amplifications with channel loss observed in [2] can be derived using an approximate loss model described by

$$H(\omega) = \exp(-k\,|\,\omega\,| - j\omega\, t_d) \quad (21)$$

where k is the loss constant and t_d the channel delay. Substitution of Eq. 21 into Eq. 9 yields the amplification factor for SJ below the jitter Nyquist frequency ω_0 as

$$F_{SJ}(\omega) = [\exp(-k\omega) + \exp(k\omega)]/2 \quad (22)$$

It can be easily shown that $F_{SJ}(\omega) \geq 1$ and jitter is amplified by lossy channels at any frequency below ω_0. Equation 22 also indicates that F_{SJ} grows exponentially with jitter frequency.

DCD and RJ amplifications within the loss model are given by substituting Eq. 21 into Eq. 10 and Eq. 13, respectively.

$$F_{DCD} = [\exp(-k\omega_0) + \exp(k\omega_0)]/2 \quad (23)$$

$$F_{RJ} = \sqrt{\frac{\exp(2k\omega_0) - \exp(-2k\omega_0)}{8k\omega_0} + \frac{1}{2}} \quad (24)$$

F_{DCD} and F_{RJ} are shown to increase exponentially with data rate. Scaling of F_{DCD} and F_{RJ} is obtained by rewriting Eqs. 23 and 24 as

$$F_{DCD} = \cosh[\ln 10 \cdot |\,D(\omega_0)\,|/20] \quad (25)$$

$$F_{RJ} = \sqrt{\frac{5}{\ln 10 \cdot |\,D(\omega_0)\,|}\sinh\left[\frac{\ln 10}{10}|\,D(\omega_0)\,|\right] + \frac{1}{2}} \quad (26)$$

where $D(\omega_0) = 20\log_{10}|H(\omega_0)|$ denotes the channel loss in dB at the fundamental frequency.

IV. COMPARISON BETWEEN THEORY AND SIMULATION

A set of four single-ended channels terminated with 50 Ohm are used in the study. Their S-parameters are generated from EM simulations. The Svensson-Dermer model [5] is employed to model the substrate loss. Simulated insertion loss is plotted in Fig. 1. The clock signal transmitted into the channel is represented by 1010 square wave. SJ, DCD and white noise Gaussian RJ are applied at transitions. The channel output signal is calculated using Eq. 14 with step responses characterized by SPICE transient simulations. One million bits are run in each simulation.

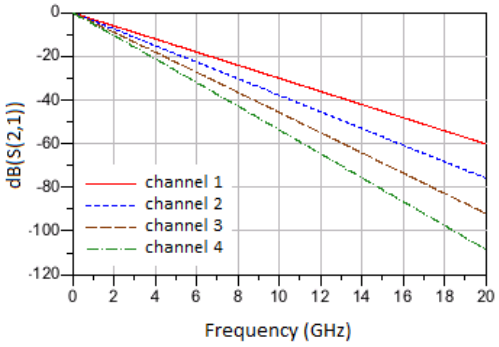

Figure 1. Channel insertion loss.

Simulated SJ amplification factors as functions of SJ frequency in channels 1 and 2 at 10 Gbps and 20 Gbps are plotted in Fig. 2. Two sets of theoretical results calculated using Eq. 9 based on S(2,1) and Eq. 22 based on the

approximate loss model described in Eq. 21 are also shown in the plot. Loss constants are extracted from slopes of insertion loss. Figure 2 shows that simulation results are in good agreement with theoretical predictions. Discrepancy between results given by Eq. 9 and Eq. 22 is small, indicating that the loss model is a reasonable approximation in these channels. Comparison of results in channel 2 at 10 Gbps and 20 Gbps suggests that F_{SJ} is insensitive to data rate in lossy channels, as predicted by Eq. 22. The amplification factor is found to be greater than or equal to one at any SJ frequency and grow exponentially with it.

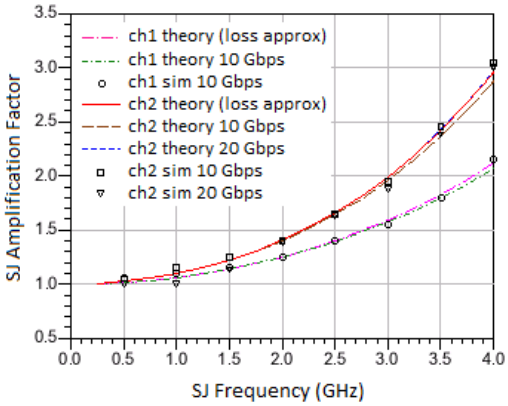

Figure 2. SJ amplification factors obtained from simulations and theoretical calculations with Eq. 9 and Eq. 22.

DCD and RJ amplification factors in channels 1 and 2 as functions of data rate are plotted in Fig. 3 and Fig. 4, respectively. For DCD, theoretical results are calculated using Eq. 10 and Eq. 23. For RJ, Eq. 13 and Eq. 24 are used. Figure 5 shows the scaling of F_{DCD} and F_{RJ} with channel insertion loss at the fundamental frequency in all channels at different data rates. The theoretical scaling is given by Eq. 25 for DCD and Eq. 26 for RJ. Agreement is found between simulation and theory in all cases. The scaling results are consistent with those reported in [2].

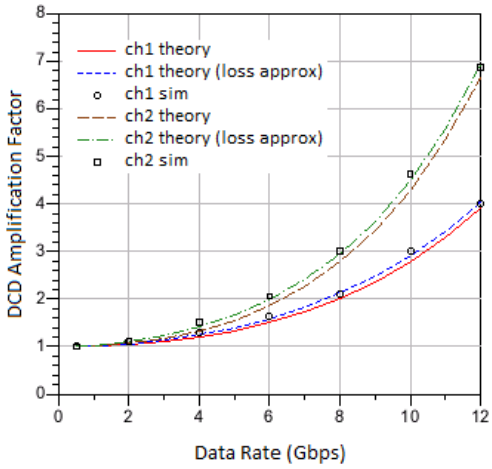

Figure 3. DCD amplification factors obtained from simulations and theoretical calculations with Eq. 10 and Eq. 23.

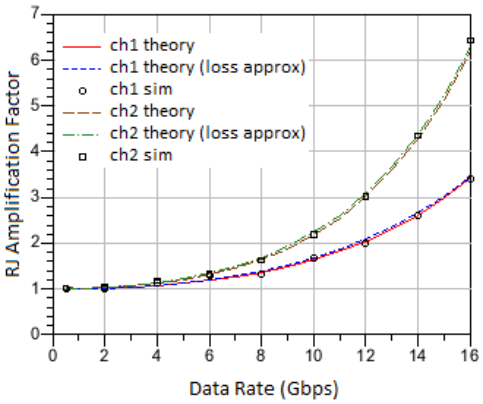

Figure 4. RJ amplification factors obtained from simulations and theoretical calculations with Eq. 13 and Eq. 24.

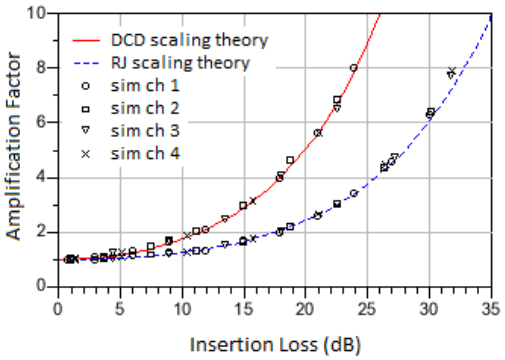

Figure 5. DCD and RJ amplification scaling with insertion loss obtained from simulations and theoretical calculations with Eq. 25 and Eq. 26. The insertion loss is at the fundamental frequency.

V. SUMMARY

In this paper clock channel jitter amplification factors in terms of transfer function or S-parameters are derived. Amplification is shown to result from the smaller loss in the jitter LSB than in the fundamental. The amplification scaling with channel loss is obtained by using an approximate loss model. In this model the amplification is found to occur at any jitter frequency. The theory is confirmed by simulation data.

REFERENCES

[1] S. Chaudhuri, W. Anderson, J. McCall, and S. Dabrai, "Jitter amplification characterization of passive clock channels at 6.4 and 9.6 Gb/s," Proc. IEEE 15th Topical Meeting on Electric Performance of Electronic Packaging, Scottsdale, AZ, Oct. 2006, pp. 21-24.

[2] C. Madden, S. Chang, D. Oh and C. Yuan, "Jitter Amplification Considerations for PCB Clock Channel Design," IEEE 16th Topical Meeting on Electr. Performance Electron. Packag., Atlanta, GA, pp. 135-138, Oct. 2007.

[3] S. Chang, D. Oh and C. Madden, "Jitter modeling in statistical link simulation," Proc. IEEE Electromagn. Compat. Symp., Detroit, MI, Aug. 18-22, 2008.

[4] F. Rao, V. Borich, H. Abebe and M. Yan, "Rigorous modeling of transmit jitter for accurate and efficient statistical eye simulation," IEC DesignCon, Feb. 2010.

[5] C. Svensson and G. Dermer, "Time domain modeling of lossy interconnects," IEEE Trans. Adv. Packaging, vol. 24, no. 2, pp. 191-196, May 2001.

www.agilent.com

Product specifications and descriptions in this document subject to change without notice.

Published in USA, November 1, 2012

5991-1255EN